Proceedings of the
47th IEEE Conference on Decision and Control
Cancun, Mexico, Dec. 9-11, 2008

Curve Tracking Control for Autonomous Vehicles with Rigidly Mounted Range Sensors

Jonghoek Kim, Fumin Zhang, and Magnus Egerstedt

Abstract— **In this paper, we present a feedback control law to make an autonomous vehicle with rigidly mounted range sensors track a desired curve. In particular, we consider a vehicle which has two range sensors that emit rays perpendicular to the velocity of the vehicle. Under such a sensor configuration, singularities are bound to occur in the feedback control law. Thus, to overcome this, we derive a hybrid strategy of switching between control laws close to the singularity.**

I. Introduction

Curve tracking control is fundamental for autonomous vehicles following desired paths, e.g. staying in lanes, or avoiding obstacles. An example in which this becomes relevant is when an autonomous vehicle is to follow the curb or the lane markings of a car. In fact, Fig.1 shows the mobile vehicle that represented Georgia Tech in the DARPA Urban Grand Challenge in 2007. As one of this vehicle's lane perception strategies, two rigidly mounted range sensors(lidars) were installed on both sides of the vehicle. At each instant of time, the vehicle emits a ray forming a fixed angle with the velocity of the vehicle. When the sensor ray intersects a lane, it detects a point on the lane. From the distance measurements taken, the autonomous vehicle estimates the curvature of the lane at the detected point, the distance from the point, and the angle between the heading direction of the vehicle and the tangent vector to the lane.

In this paper, we design a curve tracking control law that uses this information to produce the desired lane following behavior as a component in the Georgia Tech Urban Grand Challenge system. It should be noted that our results can be applied to a number of other types of autonomous vehicles with rigidly mounted range sensors.

The literature is abundant with papers on trajectory tracking for autonomous vehicles. For example, in [1], a reference point on the contour being tracked moves along the reference trajectory while the vehicle follows it. Otherwise, the reference point might stop to wait for the vehicle. In [2] and [3], a gyroscopic feedback law was used to model the interaction of a particle with an image particle representing the closest point on a closed curve bounding an obstacle. This controller design method was generalized to cooperative motion patterns on closed curves for multiple vehicles in [4], [5], [6]. The closest point is also used for path following in [7]. In [8], sensors provide measurements at different fixed points in front of the vehicle. From the data, a recursive spline is updated, then tracked by applying a suitable feedback control law. Similarly, the problem of tracking a ground curve is formulated as controlling the shape of the curve in the image plane in [9]. Other vision-based path following methods can be found in [10], [11], [12]. To achieve motion camouflage, biologically plausible feedback law which has an intuitive physical interpretation is shown in [13]. The authors of [14] determined bound of the tolerance sampling interval so that the vehicle stays in the lane. A feedback linearization approach and Lyapunov-oriented control designs are presented to make a mobile vehicle converge to a predefined path [15]. Curve tracking for atomic force microscope is considered in [16]. A decentralized coordination algorithm for multiple vehicles to locate and track a dynamic perimeter is presented in [17]. The authors of [18] proposed a control law for following isolines in a potential field not relying on higher order characteristics of the field such as the gradient at a point or the curvature of the isolines.

Fig. 1. The Sting-1 vehicle during testing at Georgia Tech.

Conditions for nonlinear switched system to be asymptotically stable were presented in [19]. In [20],[21], and [22], multiple Lyapunov functions were presented for making a switched system to be Lyapunov

Jonghoek Kim, Fumin Zhang, and Magnus Egerstedt are with the School of Electrical and Computer Engineering, Georgia Institute of Technology, USA. Email: jkim37@mail.gatech.edu, {fumin,magnus}@ece.gatech.edu

978-1-4244-3124-3/08/$25.00 ©2008 IEEE

stable. Furthermore, three composite quadratic Lyapunov functions are used for the construction of stabilizing laws for discrete-time switched systems [23]. In [24], the authors proposed control laws that switch between an approximate control law when the system is near a singularity, and an exact control law when the system is bound away from the singularity.

A similar philosophy is pursued in this paper. In fact, the control law for boundary following presented in this paper has two attractive features. First, to overcome singularities of a Lyapunov function-oriented control law, a switched controller is presented to make the system asymptotically stable. Second, our approach allows a vehicle to follow a boundary curve using only two range sensors. Hence, this approach does not require wide-angle scanning that is commonly assumed by other boundary-following algorithms.

II. Boundary-Following Model with Rigidly Mounted Range Sensors

Consider a vehicle with two range sensors that emit rays forming a fixed angle α with the velocity of the vehicle. When a boundary curve is presented in the plane, the sensor ray will intersect the boundary and detect a point $\vec{r}_2$, which will be called the *detected point*. Here, $\vec{r}_1$ is the position of the vehicle. Hence, the relative position between the vehicle and the detected point is $\vec{r}_\alpha = \vec{r}_2 - \vec{r}_1$, and ϕ is the angle measured counterclockwise from the tangent vector $\vec{x}_2$ at the detected point to the heading direction of the vehicle $\vec{x}_1$.

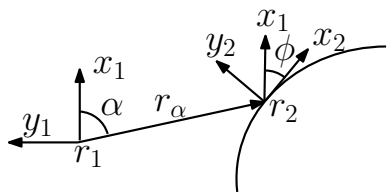

Fig. 2. A vehicle with a rigidly mounted sensor at angle α and a boundary curve in its environment.

We first establish two Frenet-Serret frames [25]: one at the vehicle, the other at the detected point, as shown in Fig. 2. These two frames satisfy the Frenet-Serret equations:

$$\begin{aligned}\dot{\vec{r}}_1 &= v_1\vec{x}_1\\ \dot{\vec{x}}_1 &= v_1 u\vec{y}_1\\ \dot{\vec{y}}_1 &= -v_1 u\vec{x}_1\end{aligned} \tag{1}$$

$$\begin{aligned}\dot{\vec{r}}_2 &= \dot{s}\vec{x}_2\\ \dot{\vec{x}}_2 &= \dot{s}\kappa\vec{y}_2\\ \dot{\vec{y}}_2 &= -\dot{s}\kappa\vec{x}_2,\end{aligned} \tag{2}$$

where v_1 is the speed control, κ is the curvature of the curve at the detected point, and s is the arc-length parameter of the curve. Here, u is the steering (i.e., curvature) control we apply to avoid colliding with the obstacle and to achieve boundary following.

We may choose the positive direction of the boundary curve such that

$$\vec{x}_1 \cdot \vec{x}_2 = \cos(\phi) > 0. \tag{3}$$

When the curve is convex, i.e., curving away from the vehicle, we have $\kappa < 0$. When the curve is concave, i.e. curving towards the vehicle, the curvature $\kappa > 0$. The above settings for the interaction between the vehicle and the boundary curve were introduced in [2].

The key idea of curve tracking control is to control the relative motion between the vehicle and the detected point. For this purpose, we develop a set of equations that govern the relative motion.

The relative position between the free particle and the detected point is ($\vec{r}_\alpha = \vec{r}_2 - \vec{r}_1$). In Fig. 2, α is defined as the angle formed by $\vec{r}_\alpha$ and $\vec{x}_1$. Also, let $r_\alpha = \|\vec{r}_\alpha\|$. Then

$$\vec{r}_\alpha \cdot \vec{x}_1 = \cos(\alpha) r_\alpha. \tag{4}$$

To derive the relative motion equations, we need to find $\dot{r}_\alpha$, $\dot{s}$ and $\dot{\phi}$.

We first obtain an equation between $\dot{r}_\alpha$ and $\dot{s}$. We take the time derivative of $\vec{r}_\alpha$ using (1) and (2) to get

$$\dot{\vec{r}}_\alpha = \dot{s}\vec{x}_2 - v_1\vec{x}_1. \tag{5}$$

Differentiating (4) with respect to time on both sides, we obtain

$$\dot{\vec{r}}_\alpha \cdot \vec{x}_1 + \vec{r}_\alpha \cdot \dot{\vec{x}}_1 = \cos(\alpha)\dot{r}_\alpha. \tag{6}$$

And then, replacing $\dot{\vec{x}}_1$ by $v_1 u\vec{y}_1$, we get

$$\dot{\vec{r}}_\alpha \cdot \vec{x}_1 + \vec{r}_\alpha \cdot v_1 u\vec{y}_1 = \cos(\alpha)\dot{r}_\alpha. \tag{7}$$

Replacing $\dot{\vec{r}}_\alpha$ in (7) by (5), we obtain

$$(\dot{s}\vec{x}_2 - v_1\vec{x}_1) \cdot \vec{x}_1 + \vec{r}_\alpha \cdot v_1 u\vec{y}_1 = \cos(\alpha)\dot{r}_\alpha. \tag{8}$$

We observe that, in Fig. 2, the angle formed by $\vec{x}_1$ and $\vec{x}_2$ is ϕ. Also, the angle formed by $\vec{r}_\alpha$ and $\vec{y}_1$ is $(\frac{\pi}{2} + \alpha)$. Therefore, we get

$$\dot{s}\cos(\phi) = v_1(1 + sin(\alpha) r_\alpha u) + \cos(\alpha)\dot{r}_\alpha. \tag{9}$$

Note that $r_\alpha^2 = \|\vec{r}_\alpha\|^2 = (\vec{r}_2 - \vec{r}_1) \cdot (\vec{r}_2 - \vec{r}_1)$, and from this it can be shown that

$$\dot{s} = \frac{v_1(r_\alpha u + \sin(\alpha))}{\sin(\alpha - \phi)}. \quad (10)$$

and

$$\dot{r}_\alpha \quad = v_1 \frac{\sin(\phi) + r_\alpha u \cos(\alpha - \phi)}{\sin(\alpha - \phi)}. \quad (11)$$

Now let us find the equation for $\dot{\phi}$. From Fig. 2, we can see that the angle between $\vec{x}_1$ and $\vec{y}_2$ is $(\frac{\pi}{2} - \phi)$. Therefore, we get

$$\sin(\phi) = \vec{x}_1 \cdot \vec{y}_2, \quad (12)$$

from which it follows that the equation for $\dot{\phi}$ is

$$\dot{\phi} \quad = v_1 r_\alpha u(\tfrac{1}{r_\alpha} - \tfrac{\kappa}{\sin(\alpha - \phi)}) - \tfrac{v_1 \sin(\alpha)\kappa}{\sin(\alpha - \phi)}. \quad (13)$$

For the Sting-I autonomous vehicle, the sensor on each side of the vehicle is installed such that $\alpha = \frac{\pi}{2}$. In this case, (10) is simplified as

$$\dot{s} = \frac{v_1(r_\alpha u + 1)}{\cos(\phi)}. \quad (14)$$

(11) is simplified as

$$\dot{r}_\alpha = v_1 \tan(\phi)(1 + r_\alpha u). \quad (15)$$

Also, (13) is simplified as

$$\dot{\phi} = v_1 u(1 - \frac{r_\alpha \kappa}{\cos(\phi)}) - \frac{\kappa v_1}{\cos(\phi)}. \quad (16)$$

The system equations are different from the equations for the closest point in [2].

III. Controller Design and Convergence Analysis

A. Lyapunov function

Consider the Lyapunov function candidate

$$V_1 = -ln(\cos(\phi)) + h(r_\alpha), \quad (17)$$

$h(r_\alpha)$ in (17) should satisfy these conditions:

1) $dh/dr_\alpha = f(r_\alpha)$,where $f(r_\alpha)$ is a Lipschitz continuous function on (0,∞), so that $h(r_\alpha)$ is continuously differentiable on (0,∞).
2) $\lim_{r_\alpha \to 0} f(r_\alpha) = -\infty$, which leads to $\lim_{r_\alpha \to 0} h(r_\alpha) = \infty$. This is needed to blow up V_1 as the moving vehicle approaches collision with the boundary curve.
3) $f(r_\alpha)$ vanishes at a point where $r_\alpha = r_0$. At which point, $h(r_\alpha)$ is also zero. This is for the moving vehicle to converge to the desired relative position at a distance from the boundary curve given by $r_\alpha = r_0$.
4) $\lim_{r_\alpha \to \infty} h(r_\alpha) = \infty$. By this condition and the form of V_1, we conclude that V_1 is radially unbounded (i. e., $V_1 \to \infty$ as $\|\phi\| \to \pi/2$, as $r_\alpha \to 0$, or as $r_\alpha \to \infty$).

Observe that V_1 given by (17) is continuously differentiable provided (3) holds. In (17), the term $-ln(\cos(\phi))$ penalizes misalignment between the tangent vector of the moving vehicle with the tangent vector to the boundary curve at the detected point. The term $h(r_\alpha)$ in (17) deals with the separation between the moving vehicle and the boundary curve. In short, V_1 is designed to make a vehicle converge to the relative position where $r_\alpha = r_0$ and $\phi = 0$. Here, r_0 represents the desired separation between the moving vehicle and the boundary curve for boundary-following. This form of Lyapunov function has been used in recent papers regarding boundary following and curve tracking using the closest point information in [2], and [6].

For the point detected by the fixed range sensors at an angle $\alpha = \pi/2$, our candidate $f(r_\alpha)$ satisfying these conditions is

$$f(r_\alpha) = \frac{-1}{r_\alpha} + \frac{1}{r_0} \quad (18)$$

where r_0 is a positive constant which represents the desired separation between the moving vehicle and the boundary curve for boundary-following. Further, the corresponding $h(r_\alpha)$ is

$$h(r_\alpha) = -\ln(r_\alpha) + \frac{r_\alpha}{r_0} + \ln(r_0) - 1, \quad (19)$$

which satisfies the conditions for $h(r_\alpha)$ in V_1 (17).

The time derivative of V_1 is

$$\dot{V}_1 = \quad -\tan(\phi)[u(\frac{v_1 r_\alpha \kappa}{\cos(\phi)} - v_1 - v_1 f(r_\alpha) r_\alpha) + \frac{v_1}{\cos(\phi)}\kappa - v_1 f(r_\alpha)], \quad (20)$$

where we have used (15), (16), and (17). We now assume that the speed $v_1 > 0$ is a constant and design steering control u so that $\dot{V}_1 \leq 0$.

B. Tracking control for convex curves

We first consider the case when the curve is convex and curving away from the vehicle. In this case we have $\kappa < 0$.

One choice of u which leads to $\dot{V}_1 \leq 0$ is

$$u_1 = \frac{v_1 \kappa - \cos(\phi)(v_1 f(r_\alpha) + \mu \sin(\phi))}{v_1(\cos(\phi) + f(r_\alpha) r_\alpha \cos(\phi) - r_\alpha \kappa)}, \quad (21)$$

where $\mu > 0$ is a constant. The time derivative of V_1 in (20) with u given by (21) is

$$\dot{V}_1 = -\mu \frac{\sin^2(\phi)}{\cos(\phi)} \leq 0, \quad (22)$$

where (3) is used. Thus, $\dot{V}_1 \leq 0$ and $\dot{V}_1 = 0$ if and only if $\sin(\phi) = 0$. But by (3), we see that $\dot{V}_1 = 0$ if and only if $\phi = 0$.

From now on, we define the case where the denominator of control law is zero as *singular case* of the controller. It *seems possible* that the control law given by (21) is singular when the denominator of u_1 equals to zero, i.e., $\cos(\phi) = \frac{r_\alpha \kappa}{1+f(r_\alpha)r_\alpha}$. Using (18), we have

$$\cos(\phi) = \frac{r_\alpha \kappa}{1 + f(r_\alpha)r_\alpha} = r_0 \kappa. \tag{23}$$

Therefore, in the case where the curvature of the lane at the detected point κ is equal to or smaller than zero in (23), the denominator of the control law in (21) will never be zero since $\cos(\phi) > 0$, and we can now state the following theorem:

Theorem 1: Consider the case where the boundary curve is convex, i.e., $\kappa < 0$. Then, using the steering control law in (21), the vehicle satisfying (3) with constant speed $v_1 > 0$ tracks the curve at a distance r_0 without collision.

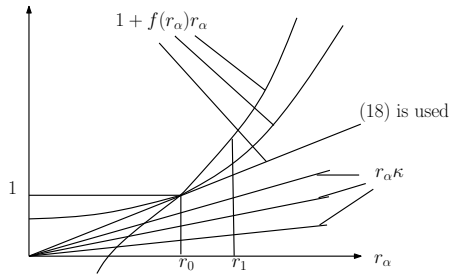

Fig. 3. Comparison of $1 + f(r_\alpha)r_\alpha$ and κr_α. Control law given by (21) is singular when $\cos(\phi) = \frac{r_\alpha \kappa}{1+f(r_\alpha)r_\alpha}$. We argue that singular case can not be removed by choosing $f(r_\alpha)$ if the curvature κ is upper bounded.

C. Control laws for concave curve with bounded curvature

We consider the case when the curve is concave, i.e. curving towards the vehicle. In this case we have $\kappa > 0$. It is possible that the control law given by (21) is singular when the denominator of u_1 equals to zero, i.e.,$\cos(\phi) = \frac{r_\alpha \kappa}{1+f(r_\alpha)r_\alpha}$. However, in the case where the curvature of the lane at the detected point κ is bigger than $\frac{1}{r_0}$ in (23), no uncontrollable case happens because $|\cos\phi| \leq 1$.

In the real experimental environment, it is necessary for the vehicle to follow a boundary curve whose curvature is sufficiently small, such as a straight line. We argue that in this case the singular case exists regardless of the choice of $f(r_\alpha)$.

Fig.3 shows possible graphs of $1 + f(r_\alpha)r_\alpha$ and $r_\alpha\kappa$ respectively. When (18) is used as $f(r_\alpha)$, we get $1 + f(r_\alpha)r_\alpha = \frac{r_\alpha}{r_0}$. Therefore, the straight line connecting the origin and (r_0,1) represents $1+f(r_\alpha)r_\alpha$ when (18) is used as $f(r_\alpha)$. In Fig.3, regardless of $f(r_\alpha)$, $1+f(r_\alpha)r_\alpha$ is a continuous function which is equal to 1 when $r_\alpha = r_0$. Also, regardless of the decreasing rate of $f(r_\alpha)$ as $r_\alpha \downarrow 0$, we can assure that $\lim_{r_\alpha \downarrow 0} 1 + f(r_\alpha)r_\alpha \leq 1$. As $r_\alpha \downarrow r_0$, we see that $f(r_\alpha)$ and r_α both decrease to make $(1 + f(r_\alpha)r_\alpha)$ decrease for any choice of $f(r_\alpha)$.

At the same time, the possible $r_\alpha\kappa$ are plotted as the straight lines. If the curvature κ is upper bounded by $\frac{1}{r_0}$, then these straight lines will be below the curve that represents $(1 + f(r_\alpha)r_\alpha)$, regardless of what $f(r_\alpha)$ is. Therefore, $\frac{r_\alpha \kappa}{1+f(r_\alpha)r_\alpha} < 1$ and $\cos\phi = \frac{r_\alpha \kappa}{1+f(r_\alpha)r_\alpha}$ always has a solution for ϕ. This singular case can not be removed by choosing $f(r_\alpha)$.

D. The safety zone

As seen on the form of (23), singular case will never happen if $|\phi| < \arccos(r_0\kappa_M)$, where κ_M is the upper bound of κ. Thus, we define the set $U = \{(r_\alpha, \phi)|V_1(r_\alpha, \phi) < -ln(|r_0\kappa_M|)\}$ as the *safety zone*. The controller (21) is used inside the safety zone. Since this controller yields $\dot{V}_1 \leq 0$, we conclude that once the vehicle under control enters the safety zone U, it will never leave. Therefore, according to Theorem 1, the curve tracking behavior is stabilized without collision.

E. Switching control that aims for the safety zone

When the vehicle is initially out of the safety zone but, during its movements, it will come close to the set where $\cos(\phi) = r_0\kappa$, control law (21) can not be applied due to singularity.

We develop a switching system as depicted in Fig.4 to steer the system into the safety zone in finite time. Four cases are distinguished, which correspond to four sets G_1, G_2, G_3 and G_4 defined as follows:

$$\begin{aligned} G_1 &= \{(r_\alpha, \phi)|\|\cos(\phi) - r_0\kappa\| > \epsilon \text{ but } (r_\alpha, \phi) \notin U\} \\ G_2 &= \{(r_\alpha, \phi)|\epsilon_2 < \|\cos(\phi) - r_0\kappa\| \leq \epsilon\} \\ G_3 &= \{(r_\alpha, \phi)|\|\cos(\phi) - r_0\kappa\| \leq \epsilon_2\} \\ G_4 &= U, \end{aligned} \tag{24}$$

where $\epsilon_2 < \epsilon$.

Three control laws are designed for these four cases. When the system states are in G_1 or G_4, we use u_1 in (21). When the states enter G_2 from G_1, we switch to u_2 which is

$$u_2 = \frac{v_1\kappa - \cos(\phi)(v_1 f(r_\alpha) + \mu_2 \sin(\phi))}{v_1(\cos(\phi) + f(r_\alpha)r_\alpha \cos(\phi) - r_\alpha\kappa)}, \tag{25}$$

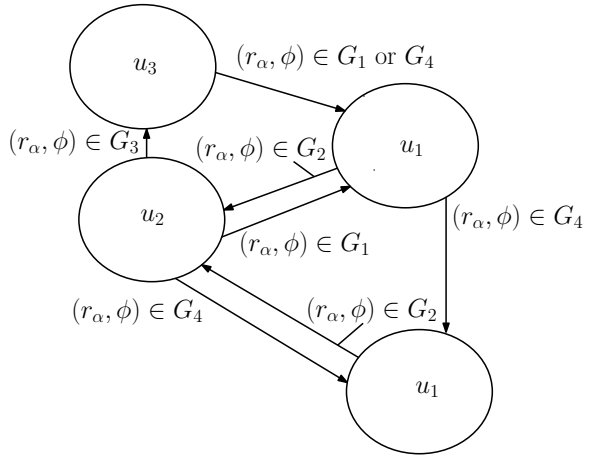

u_1	$u_1 = \frac{v_1\kappa - \cos(\phi)(v_1 f(r_\alpha) + \mu \sin(\phi))}{v_1(\cos(\phi) + f(r_\alpha) r_\alpha \cos(\phi) - r_\alpha \kappa)}$.
u_2	$u_2 = \frac{v_1\kappa - \cos(\phi)(v_1 f(r_\alpha) + \mu_2 \sin(\phi))}{v_1(\cos(\phi) + f(r_\alpha) r_\alpha \cos(\phi) - r_\alpha \kappa)}$.
u_3	$u_3 = \frac{-\mu_3 \sin(\phi) + \kappa v_1 r_\alpha}{v_1 r_\alpha(\cos(\phi) - r_\alpha \kappa)}$.

Fig. 4. The switching control strategy used to enter safety zone. u_1 in (21) is used in normal situations i.e. when the states are in G_1 or G_4. We switch to u_2 in (25) when the states enter G_2 and switch to u_3 in (27) when the states enter G_3.

where the only difference between u_1 and u_2 is that the gain μ_2 is much bigger than μ. The time derivative of V_1 under control u_2 given by (25) is

$$\dot{V}_1 = -\mu_2 \frac{\sin^2(\phi)}{\cos(\phi)} \leq 0. \tag{26}$$

When the states of the system enter G_3 from G_2 $(r_\alpha, \phi) \in G_3$, we switch to controller u_3:

$$u_3 = \frac{-\mu_3 \sin(\phi) + \kappa v_1 r_\alpha}{v_1 r_\alpha(\cos(\phi) - r_\alpha \kappa)}, \tag{27}$$

where $\mu_3 > 0$ is a constant. Under this controller, we have

$$\dot{\phi} = -\frac{\mu_3 \tan(\phi)}{r_\alpha}. \tag{28}$$

Hence, $\phi \to 0$ as $t \to \infty$. This implies that the system states will get out of G_3 and then out of G_2 in finite time. We switch back to controller u_1 after the states enter either G_1 or G_4. Note that by Theorem 1, once the states enter G_4, they will stay in G_4 and converge to the desired values.

We now prove convergence of the system under the switching control laws illustrated in Fig. 4. The idea is that the value of the Lyapunov function V_1 may be increasing under controller u_3, but such increase will be compensated by controller u_2. Hence the overall effect is that the Lyapunov function decreases until the system reaches G_4. Some notations and technical conditions are needed to rigorously state and prove the results.

It is uninteresting if the states never enters the set G_3. In which case V_1 would be decreasing until G_4 is reached. Therefore, we discuss the most general case i.e. the states of the system enters G_3 for a number of times. In order to enter G_3, the system must enter G_2 first. We use the notations t_1^i to indicate the time when the system enters G_2, t_2^i to indicate the time when the system enters G_3, and t_3^i to indicate the time when the system leaves G_2. The index i is used to distinguish multiple entries. If the states enter G_3 and later leaves G_2, then t_1^i, t_2^i and t_3^i happen in sequence.

The following technical assumptions are needed

(A1) The curvature κ is bounded above by $\kappa_M > 0$.
(A2) The desired distance r_0 satisfies that $r_0 \kappa_M < 1$.
(A3) Define ζ as $v_1 \| -arccos(\kappa_M r_0 + \epsilon) + arccos(\kappa_M r_0 - \epsilon_2) \| + \epsilon_3$, where $\epsilon_3 > 0$ is a constant. We assume that the gains μ_2 and μ_3 in controllers u_2 and u_3 satisfy $\mu_2 \mu_3 (t_2^i - t_1^i) > \frac{\zeta r_0 \kappa_M}{1 - (r_0 \kappa_M)^2}$ for all i.

Assumptions (A1) and (A2) put mild constraints on the curve to follow. Assumption (A3) is the key technical assumption. This assumption can always be satisfied when $t_2^i - t_1^i \neq 0$ and if we allow the gains μ_2 or μ_3 to be arbitrarily large.

Theorem 2: Consider the system defined by (15) and (16) governing the relative distance and heading angle between the vehicle and the detected point. Suppose the vehicle travels at constant speed v_1. Under the switching strategy in Fig. 4, with assumptions (A1)-(A3) satisfied, the states of the switching closed loop system enter G_4 in finite time.

We omit the proof of this theorem, but note that it should be organized along two steps, namely

1) Show that when u_3 is used, V_1 will increase a finite amount bounded above in the worst case.
2) Show that when u_2 is used, V_1 will decrease more than the upper bound for its increase under u_3.

In Fig.5, a typical switching process is plotted. Controller u_1 is used from 0 to t_1^i, u_2 is used from t_1^i to t_2^i, u_3 is used from t_2^i to t_3^i, and u_1 is used again after t_3^i. Intervals of using u_2 is long enough to overcome the increase of V_1 inside the interval when u_3 is used. V_1 always decrease more than it increases.

In the case where $r_\alpha = r_0$ and $\cos(\phi) = r_0 \kappa$, we have singular cases of u_1, u_2 and u_3 at the same time. This singular case will not happen if the vehicle is in the safety zone. An example of applying the switched

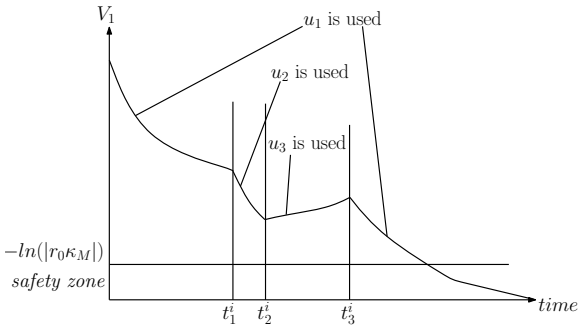

Fig. 5. The Lyapunov function V_1 in a typical case of switching control. u_1 in (21) is used from 0 to t_1^i, u_2 in (25) is used from t_1^i to t_2^i, u_3 in (27) is used from t_2^i to t_3^i, and u_1 is used from t_3^i to final time.

control strategy is shown in Fig 6, in which switches are needed to overcome the singular case.

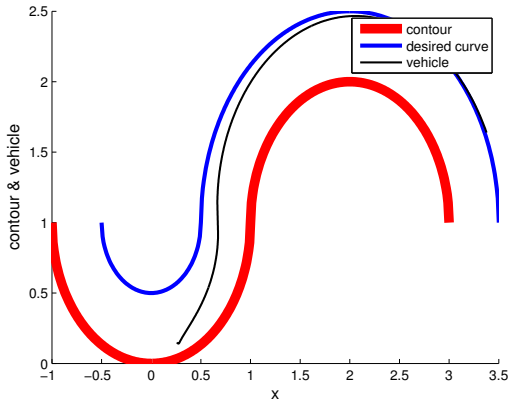

Fig. 6. The vehicle is close to the set where $\cos(\phi) = \kappa r_0$ initially. However, switched control strategy is used to overcome the singular case.

REFERENCES

[1] M. Egerstedt, X. Hu, and A. Stotsky, "Control of mobile platforms using a virtual vehicle approach," vol. 46, pp. 1777–1782, November 2001.

[2] F. Zhang, E. Justh, and P. S. Krishnaprasad, "Boundary following using gyroscopic control," in *Proc. of 43rd IEEE Conf. on Decision and Control*. Atlantis, Paradise Island, Bahamas: IEEE, 2004, pp. 5204–5209.

[3] F. Zhang, A. O'Connor, D. Luebke, and P. S. Krishnaprasad, "Experimental study of curvature-based control laws for obstacle avoidance," in *Proceedings of 2004 IEEE International Conf. on Robotics and Automation*. New Orleans, LA: IEEE, 2004, pp. 3849–3854.

[4] F. Zhang and N. E. Leonard, "Coordinated patterns of unit speed particles on a closed curve," *Systems and Control Letters*, vol. 56, no. 6, pp. 397–407, 2007.

[5] F. Zhang, E. Fiorelli, and N. E. Leonard, "Exploring scalar fields using multiple sensor platforms: Tracking level curves," in *Proc. of 46th IEEE Conf. on Decision and Control*, New Orleans, LA, 2007, pp. 3579–3584.

[6] F. Zhang, D. M. Fratantoni, D. Paley, J. Lund, and N. E. Leonard, "Control of coordinated patterns for ocean sampling," *International Journal of Control*, vol. 80, no. 7, pp. 1186–1199, 2007.

[7] C. Samson, "Control of chained systems: Application to path-following and time-varying point-stabilization of mobile robots," *IEEE Trans. on Automatic Control*, vol. 40, no. 1, pp. 64–77, 1995.

[8] R. Frezza and G. Picci, "On line path following by recursive spline updating," in *Proc. of the 34th Conf. on Decision and Control*, ser. 13-15, vol. 4, New Orleans, December 1995, pp. 4047 – 4052.

[9] Y. Ma, J. Koseck'a, and S. Sastry, "Vision guided navigation for a nonholonomic mobile robot," in *Proc. of the 36th IEEE Conference on Decision and Control*, ser. 10-12, vol. 3, December 1997, pp. 3069 – 3074.

[10] E. D. Dickmanns and V. Graefe, "Applications of dynamic monocular machine vision," *Machine Vision and Applications*, vol. 1, no. 4, pp. 241–261, 1988.

[11] E. D. Dickmanns and B. D. Mysliwetz, "Recursive 3-d road and relative ego-state estimation," *IEEE Transactions on Pattern Analysis and Machine Intelligence*, vol. 14, no. 2, pp. 199–213, 1992.

[12] D. Raviv and M. Herman, "A nonreconstruction approach for road following," *Proc. of SPIE: Intelligent Robots and Computer Vision*, vol. 1608, no. 5, pp. 2–12, 1992.

[13] E. W. Justh and P. S. Krishnaprasad, "Steering laws for motion camouflage," *Royal Society of London Proceedings Series A*, vol. 462, pp. 3629–3643, Dec. 2006.

[14] K.Li and J.Baillieul, "Data-rate requirements for nonlinear feedback control," in *Proc. 6th IFAC Symp. Nonlinear Contr. Sys.*, Uni.Stuttgart, Germany, 2004, pp. 1277–1282.

[15] A. Micaelli and C. Samson, "Trajectory tracking for unicycle-type and two-steering-wheels mobile robots," INRIA, Tech. Rep. RR-2097, November 1993.

[16] S. B. Andersson and J. Park, "Tip steering for fast imaging in AFM," in *Proc. 2005 American Control Conf.*, Portland, OR, June 6-10, 2005, pp. 2469–2474.

[17] J. Clark and R. Fierro, "Cooperative hybrid control of robotic sensors for perimeter detection and tracking." 2005 American Control Conference, 2005, pp. 3500 – 3505.

[18] D. Baronov and J. Baillieul, "Reactive exploration through following isolines in a potential field," in *American Control Conference*, July 2007, pp. 2141 – 2146.

[19] J.P.Hespanha and A.S.Morse, "Stability of switched systems with average dwell-time," in *Proceedings 38th Conference on Decision and Control*, vol. 3, 1999, pp. 2655 – 2660.

[20] D. Liberzon and A. S. Morse, "Benchmark problems in stability and design of switched systems," IEEE Control Systems Magazine, Tech. Rep., October 1999.

[21] M. Branicky, "Multiple lyapunov functions and other analysis tools for switched and hybrid systems," in *IEEE Trans. Automatic Control*, vol. 43(4), April 1998, pp. 475–482.

[22] S. P. R. DeCarlo, M.S. Branicky and B. Lennartson, "Perspectives and results on the stability and stabilizability of hybrid systems," in *Proceedings of the IEEE*, vol. 88(2), July 2000, pp. 1069–1082.

[23] T. Hu, "Switching law construction for discrete-time systems via composite quadratic functions." 2007 American Control Conference, 2007, pp. 675 – 680.

[24] C. Tomlin and S. Sastry, "Switching through singularities," in *Proceedings of the 36th IEEE Conference on Decision and Control*, vol. 1, December 1997, pp. 1–6.

[25] M. D. Carmo, *Differential Geometry of Curves and Surfaces*. Prentice Hall, 1976.